

# A Three Site Higgsless Model

---

**R. Sekhar Chivukula, Baradhwaj Coleppa, Stefano Di Chiara, and Elizabeth H. Simmons**

*Department of Physics and Astronomy, Michigan State University*

*East Lansing, MI 48824, USA*

*E-mail: sekhar@msu.edu, baradwa@msu.edu, dichiara@msu.edu, esimmons@msu.edu*

**Hong-Jian He**

*Center for High Energy Physics, Tsinghua University*

*Beijing 100084, China*

*E-mail: hjhe@mail.tsinghua.edu.cn*

**Masafumi Kurachi**

*C.N. Yang Institute for Theoretical Physics, State University of New York*

*Stony Brook, NY 11794, USA*

*E-mail: masafumi.kurachi@stonybrook.edu*

**Masaharu Tanabashi**

*Department of Physics, Tohoku University*

*Sendai 980-8578, Japan*

*E-mail: tanabash@tuhep.phys.tohoku.ac.jp*

**ABSTRACT:** We analyze the spectrum and properties of a highly-deconstructed Higgsless model with only three sites. Such a model contains sufficient complexity to incorporate interesting physics issues related to fermion masses and electroweak observables, yet remains simple enough that it could be encoded in a Matrix Element Generator program for use with Monte Carlo simulations. We analyze the form of the fermion Yukawa couplings required to produce the ideal fermion delocalization that causes tree-level precision electroweak corrections to vanish. We discuss the size of one-loop corrections to  $b \rightarrow s\gamma$ , the weak-isospin violating parameter  $\Delta\rho$  and to the decay  $Z \rightarrow b\bar{b}$ . We find that the extra fermiophobic vector states (the analogs of the gauge-boson KK modes in a continuum model) can be reasonably light, with a mass as low as 380 GeV, while the extra (approximately vectorial) quark and lepton states (the analogs of the fermion KK modes) must be heavier than 1.8 TeV.

July 10, 2006

**KEYWORDS:** Dimensional Deconstruction, Electroweak Symmetry Breaking, Higgsless Theories, Fermion Delocalization, Multi-gauge-boson vertices, Chiral Lagrangian.

## 1. Introduction

Higgsless models [1] literally break the electroweak symmetry without invoking a scalar Higgs boson [2]. Among the most popular are models [3, 4, 5, 6] based on a five-dimensional  $SU(2) \times SU(2) \times U(1)$  gauge theory in a slice of Anti-deSitter space, with electroweak symmetry breaking encoded in the boundary conditions of the gauge fields. The spectrum includes states identified with the photon,  $W$ , and  $Z$ , and also an infinite tower of additional massive vector bosons (the higher Kaluza-Klein or  $KK$  excitations), whose exchange unitarizes longitudinal  $W$  and  $Z$  boson scattering [7, 8, 9, 10]. The properties of Higgsless models may be studied [11, 12, 13, 14, 15, 16, 17] by using the technique of deconstruction [18, 19] and computing the precision electroweak parameters [20, 21, 22, 23, 24] in a related linear moose model [25].

Our analysis of the leading electroweak parameters in a very general class of linear moose models concluded [17] that a Higgsless model with localized fermions cannot simultaneously satisfy unitarity bounds and provide acceptably small precision electroweak corrections unless it includes light vector bosons other than the photon,  $W$ , and  $Z$ . Others proposed [26, 27, 28, 29] that delocalizing fermions within the extra dimension could reduce electroweak corrections. In deconstructed language, delocalization means allowing fermions to derive electroweak properties from more than one site on the lattice of gauge groups [30, 31]. We then showed [32] for an arbitrary Higgsless model that choosing the probability distribution of the delocalized fermions to be related to the wavefunction of the  $W$  boson makes the three  $(\hat{S}, \hat{T}, W)$  of the leading zero-momentum precision electroweak parameters defined by Barbieri, et. al. [23, 24] vanish at tree-level. We denote such fermions as “ideally delocalized”. We subsequently provided a continuum realization of ideal delocalization that preserves the characteristic of vanishing precision electroweak corrections up to subleading order [33]. In the absence of precision electroweak corrections, the strongest constraints on higgsless models come from limits on deviations in multi-gauge-boson vertices; we computed the general form of the triple and quartic gauge boson couplings for these models and related them to the parameters of the electroweak chiral Lagrangian [34, 35].

In this paper, we show that many issues of current interest, such as ideal fermion delocalization and the generation of fermion masses (including the top quark mass) can be usefully illustrated in a Higgsless model deconstructed to just three sites. The Moose describing the model has only one “interior”  $SU(2)$  group and there is, accordingly, only a single triplet of  $W'$  and  $Z'$  states instead of the infinite tower of triplets present in the continuum limit. This model contains sufficient complexity to incorporate the interesting physics issues, yet remains simple enough that it could be encoded in a Matrix Event Generator program in concert with a Monte Carlo Event Generator <sup>1</sup> for a detailed investigation of collider signatures.

The three-site model we introduce here has a standard color group and an extended  $SU(2) \times SU(2) \times U(1)$  electroweak gauge group. In the next two sections, we describe the electroweak and fermionic sectors of the three-site model and then solve for the masses and wavefunctions of the particles in the spectrum: a photon, a nearly-standard  $W$  and  $Z$ , a much

---

<sup>1</sup>See e.g. those appearing on <http://www-theory.lbl.gov/tools/>.

heavier  $W'$  and  $Z'$ , a set of SM-like fermions, and heavy copies of those fermions. Sections 4 and 5 explore the couplings of the charged and neutral gauge bosons to fermions and to one another. The light fermions are ideally delocalized so that the absence of their couplings to the  $W'$  and  $Z'$  minimizes the values of electroweak precision observables. The top quark, on the other hand, is treated separately in order to provide for its large mass. Multiple gauge vertices and chiral Lagrangian parameters are studied next; given the vanishing electroweak corrections and the fermiophobic nature of the  $W'$  and  $Z'$ , they offer the best prospects for additional experimental constraints on the three-site model. The paper moves on to a discussion of the rho-parameter and  $Zb\bar{b}$  vertex at one loop. Having established that the heavy fermions must have masses of over 1.8 TeV, we discuss the structure of a low-energy effective theory in which those fermions have been integrated out. Section 9 presents our conclusions.

## 2. Three Site Model

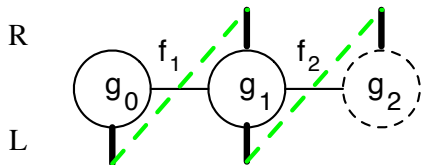


**Figure 1:** The three site model analyzed in this paper. The solid circles represent  $SU(2)$  gauge groups, with coupling strengths  $g_0$  and  $g_1$ , and the dashed line is a  $U(1)$  gauge group with coupling  $g_2$ . The left-handed fermions, denoted by the lower vertical lines, are located at sites 0 and 1, and the right-handed fermions, denoted by the upper vertical lines, at sites 1 and 2. The dashed green lines correspond to Yukawa couplings, as described in the text. As discussed below, we will take  $f_1 = f_2 = \sqrt{2}v$ , denote  $g_0 = g$ ,  $g_1 = \tilde{g}$ ,  $g_2 = g'$  and take  $\tilde{g} \gg g, g'$ .

The electroweak sector of the three-site Higgsless model analyzed in this paper is illustrated in figure 1 using “moose notation” [25]. The model incorporates an  $SU(2) \times SU(2) \times U(1)$  gauge group, and 2 nonlinear  $(SU(2) \times SU(2))/SU(2)$  sigma models in which the global symmetry groups in adjacent sigma models are identified with the corresponding factors of the gauge group. The symmetry breaking between the middle  $SU(2)$  and the  $U(1)$  follows an  $SU(2)_L \times SU(2)_R/SU(2)_V$  symmetry breaking pattern with the  $U(1)$  embedded as the  $T_3$ -generator of  $SU(2)_R$ .

The left-handed fermions are  $SU(2)$  doublets coupling to the groups at the first two sites, and which we will correspondingly label  $\psi_{L0}$  and  $\psi_{L1}$ . The right-handed fermions are an  $SU(2)$  doublet at site 1,  $\psi_{R1}$ , and two singlet fermions, denoted in figure 1 as “residing” at site 2,  $u_{R2}$  and  $d_{R2}$ . The fermions  $\psi_{L0}$ ,  $\psi_{L1}$ , and  $\psi_{R1}$  have  $U(1)$  charges typical of the left-handed doublets in the standard model,  $+1/6$  for quarks and  $-1/2$  for leptons. Similarly, the fermion  $u_{R2}$  has  $U(1)$  charges typical for the right-handed up-quarks ( $+2/3$ ), and the  $d_{R2}$  the  $U(1)$  charge associated with the right-handed down-quarks ( $-1/3$ ) or the leptons ( $-1$ ). With these assignments, we may write the Yukawa

couplings and fermion mass<sup>2</sup> term

$$\mathcal{L}_f = \lambda f_1 \bar{\psi}_{L0} \Sigma_1 \psi_{R1} + \sqrt{2} \tilde{\lambda} v \bar{\psi}_{R1} \psi_{L1} + f_2 \bar{\psi}_{L1} \Sigma_2 \begin{pmatrix} \lambda'_u \\ \lambda'_d \end{pmatrix} \begin{pmatrix} u_{R2} \\ d_{R2} \end{pmatrix} + h.c. \quad (2.1)$$

Here we have chosen to write the  $\bar{\psi}_{R1} \psi_{L1}$  Dirac mass in the form of a Yukawa coupling, for convenience, and the matrices  $\Sigma_{1,2}$  are the nonlinear sigma model fields associated with the  $f_{1,2}$  links of the moose. The Yukawa couplings introduced here are of precisely the correct form required to implement a deconstruction of a five-dimensional fermion with chiral boundary conditions [36].

It is straightforward to incorporate quark flavor and mixing in a minimal way. Adding generational indices to each of the fermion fields, we may choose the coupling  $\lambda$  and the mass term  $\sqrt{2} \tilde{\lambda} v$  to be generation-diagonal. In this case, all of the nontrivial flavor structure is embedded in the Yukawa matrices  $\lambda'_u$  and  $\lambda'_d$  – precisely as in the standard model; the only mixing parameters that appear are the ordinary CKM angles and phase. We focus most of our attention, in this paper, on the top-bottom quark doublet and their heavy partners, and we note where results for the other fermions differ.

For simplicity, we examine the case

$$f_1 = f_2 = \sqrt{2} v, \quad (2.2)$$

and work in the limit

$$x = g_0/g_1 \ll 1, \quad y = g_2/g_1 \ll 1, \quad (2.3)$$

in which case we expect a massless photon, light  $W$  and  $Z$  bosons, and a heavy set of bosons  $W'$  and  $Z'$ . Numerically, then,  $g_{0,2}$  are approximately equal to the standard model  $SU(2)_W$  and  $U(1)_Y$  couplings, and we therefore denote  $g_0 \equiv g$  and  $g_2 \equiv g'$ , and define an angle  $\theta$  such that

$$\frac{g'}{g} = \frac{\sin \theta}{\cos \theta} \equiv \frac{s}{c}, \quad (2.4)$$

In addition, we denote  $g_1 \equiv \tilde{g}$ .

In what follows, we will show that ideal mixing requires the flavor-independent mass contribution from  $\Sigma_1$  to be much smaller than the Dirac mass contribution:

$$\varepsilon_L \equiv \frac{\lambda}{\tilde{\lambda}} = \mathcal{O}(x) \ll 1, \quad (2.5)$$

While we will not immediately require that the flavor-dependent mass contributions associated with  $\Sigma_2$

$$\varepsilon_{uR,dR} \equiv \frac{\lambda'_{u,d}}{\lambda}, \quad (2.6)$$

be similarly small, we will ultimately find that they are bounded from above. The Yukawa and fermion mass terms in the Lagrangian can now be rephrased as

$$\mathcal{L}_f = \sqrt{2} \tilde{\lambda} v \left[ \varepsilon_L \bar{\psi}_{L0} \Sigma_1 \psi_{R1} + \bar{\psi}_{R1} \psi_{L1} + \bar{\psi}_{L1} \Sigma_2 \begin{pmatrix} \varepsilon_{uR} \\ \varepsilon_{dR} \end{pmatrix} \begin{pmatrix} u_{R2} \\ d_{R2} \end{pmatrix} + h.c. \right] \quad (2.7)$$

for easy reference.

<sup>2</sup>In this paper, we will not address the issue of nonzero neutrino masses. Our focus, instead, is on the physics related to the generation of the large top-quark mass.

### 3. Masses and Eigenstates

This section presents the mass eigenvalues and the wavefunctions of the gauge bosons<sup>3</sup> and fermions of the three-site model.

#### 3.1 Charged Gauge Bosons

The charged gauge-boson mass-squared matrix may be written in terms of the small parameter  $x$  as

$$\frac{\tilde{g}^2 v^2}{2} \begin{pmatrix} x^2 & -x \\ -x & 2 \end{pmatrix}. \quad (3.1)$$

Diagonalizing this matrix perturbatively in  $x$ , we find the light eigenvalue

$$M_W^2 = \frac{g^2 v^2}{4} \left[ 1 - \frac{x^2}{4} + \frac{x^6}{64} + \dots \right], \quad (3.2)$$

and the corresponding eigenstate

$$\begin{aligned} W^\mu &= v_W^0 W_0^\mu + v_W^1 W_1^\mu \\ &= \left( 1 - \frac{x^2}{8} - \frac{5x^4}{128} + \dots \right) W_0^\mu + \left( \frac{x}{2} + \frac{x^3}{16} - \frac{9x^5}{256} + \dots \right) W_1^\mu, \end{aligned} \quad (3.3)$$

where  $W_{0,1}$  are the gauge bosons associated with the  $SU(2)$  groups at sites 0 and 1. Note that the light  $W$  is primarily located at site 0.

The heavy eigenstate has an eigenvector orthogonal to that in eqn. (3.3) and a mass

$$M_{W'}^2 = \tilde{g}^2 v^2 \left[ 1 + \frac{x^2}{4} + \frac{x^4}{16} + \dots \right], \quad (3.4)$$

Comparing eqns. (3.2) and (3.4), we find

$$\frac{M_W^2}{M_{W'}^2} = \frac{x^2}{4} - \frac{x^4}{8} + \frac{x^6}{64} + \dots, \quad (3.5)$$

or, equivalently,

$$\left( \frac{g_0}{g_1} \right)^2 \equiv x^2 = 4 \left( \frac{M_W^2}{M_{W'}^2} \right) + 8 \left( \frac{M_W^2}{M_{W'}^2} \right)^2 + 28 \left( \frac{M_W^2}{M_{W'}^2} \right)^3 + \dots \quad (3.6)$$

which confirms that the  $W'$  boson is heavy in the limit of small  $x$ .

---

<sup>3</sup>Ref. [11] has previously discussed the gauge boson eigenfunctions, but wrote them in terms of the parameters  $e$ ,  $M_W$ ,  $M_Z$ ,  $M_{W'}$ , and  $M_{Z'}$ .

### 3.2 Neutral Gauge Bosons

The neutral bosons' mass-squared matrix is

$$\frac{\tilde{g}^2 v^2}{2} \begin{pmatrix} x^2 & -x & 0 \\ -x & 2 & -xt \\ 0 & -xt & x^2 t^2 \end{pmatrix}, \quad (3.7)$$

where  $t \equiv \tan \theta = s/c$ . This matrix has a zero eigenvalue, corresponding to the massless photon, with an eigenstate which may be written

$$A^\mu = \frac{e}{g} W_0^\mu + \frac{e}{\tilde{g}} W_1^\mu + \frac{e}{g'} B^\mu, \quad (3.8)$$

where  $W_{0,1}$  are the gauge bosons associated with the  $SU(2)$  groups at sites 0 and 1, the  $B$  is the gauge boson associated with the  $U(1)$  group at site 2, and the electric charge  $e$  satisfies

$$\frac{1}{e^2} = \frac{1}{g^2} + \frac{1}{\tilde{g}^2} + \frac{1}{g'^2}. \quad (3.9)$$

The light neutral gauge boson, which we associate with the  $Z$ , has a mass

$$M_Z^2 = \frac{g^2 v^2}{4c^2} \left[ 1 - \frac{x^2 (c^2 - s^2)^2}{4c^2} + \frac{x^6 (c^2 - s^2)^4}{64c^6} + \dots \right], \quad (3.10)$$

with a corresponding eigenvector

$$Z^\mu = v_Z^0 W_0^\mu + v_Z^1 W_1^\mu + v_Z^2 B^\mu \quad (3.11)$$

$$v_Z^0 = c - \frac{x^2 c^3 (1 + 2t^2 - 3t^4)}{8} + \dots \quad (3.12)$$

$$v_Z^1 = \frac{xc(1-t^2)}{2} + \frac{x^3 c^3 (1-t^2)^3}{16} + \dots \quad (3.13)$$

$$v_Z^2 = -s - \frac{x^2 s c^2 (3 - 2t^2 - t^4)}{8} + \dots \quad (3.14)$$

The heavy neutral boson has a mass

$$M_{Z'}^2 = \tilde{g}^2 v^2 \left[ 1 + \frac{x^2}{4c^2} + \frac{x^4 (1-t^2)^2}{16} + \dots \right], \quad (3.15)$$

with the corresponding eigenvector

$$Z'^\mu = v_{Z'}^0 W_0^\mu + v_{Z'}^1 W_1^\mu + v_{Z'}^2 B^\mu \quad (3.16)$$

$$v_{Z'}^0 = -\frac{x}{2} - \frac{x^3 (1-3t^2)}{16} + \dots \quad (3.17)$$

$$v_{Z'}^1 = 1 - \frac{x^2 (1+t^2)}{8} + \dots \quad (3.18)$$

$$v_{Z'}^2 = -\frac{xt}{2} + \frac{x^3 t (3-t^2)}{16} + \dots \quad (3.19)$$

### 3.3 Fermions

Next, we consider the fermion mass matrix

$$M_{u,d} = \sqrt{2}\tilde{\lambda}v \begin{pmatrix} \varepsilon_L & 0 \\ 1 & \varepsilon_{uR,dR} \end{pmatrix} \equiv \begin{pmatrix} m & 0 \\ M & m'_{u,d} \end{pmatrix}. \quad (3.20)$$

The notation introduced at the far right is used to emphasize the “see-saw” form of the mass matrix. In what follows, we will largely be interested in the top- and bottom-quarks, and therefore in  $\varepsilon_{tR}$  and  $\varepsilon_{bR}$  (or, equivalently, in  $m'_t/M$  and  $m'_b/M$ ).

Diagonalizing the top-quark seesaw-style mass matrix perturbatively in  $\varepsilon_L$ , we find the light eigenvalue

$$m_t = \frac{\sqrt{2}\tilde{\lambda}v\varepsilon_L\varepsilon_{tR}}{\sqrt{1+\varepsilon_{tR}^2}} \left[ 1 - \frac{\varepsilon_L^2}{2(\varepsilon_{tR}^2+1)^2} + \dots \right], \quad (3.21)$$

$$\approx \frac{m m'_t}{\sqrt{M^2 + m_t'^2}}. \quad (3.22)$$

Note that this is precisely the same form as found in [29]. For the bottom-quark, we find the same expression with  $\varepsilon_{tR} \rightarrow \varepsilon_{bR}$ , and therefore (neglecting higher order terms in  $\varepsilon_{bR}^2$ )

$$\frac{m_b}{m_t} \approx \frac{\varepsilon_{bR}}{\varepsilon_{tR}} \sqrt{1 + \varepsilon_{tR}^2} \quad (3.23)$$

The heavy eigenstate ( $T$ ) corresponding to the top-quark has a mass

$$m_T = \sqrt{2}\tilde{\lambda}v\sqrt{1+\varepsilon_{tR}^2} \left[ 1 + \frac{\varepsilon_L^2}{2(\varepsilon_{tR}^2+1)^2} + \dots \right], \quad (3.24)$$

$$\approx \sqrt{M^2 + m_t'^2} \quad (3.25)$$

and similarly for the heavy eigenstate corresponding to the bottom-quark ( $B$ ) with  $\varepsilon_{tR} \rightarrow \varepsilon_{bR}$  (or, equivalently,  $m'_t \rightarrow m'_b$ ).

The left- and right-handed light mass eigenstates of the top quark are

$$\begin{aligned} t_L &= t_L^0 \psi_{L0}^t + t_L^1 \psi_{L1}^t \\ &= \left( -1 + \frac{\varepsilon_L^2}{2(1+\varepsilon_{tR}^2)^2} + \frac{(8\varepsilon_{tR}^2-3)\varepsilon_L^4}{8(\varepsilon_{tR}^2+1)^4} + \dots \right) \psi_{L0}^t + \left( \frac{\varepsilon_L}{1+\varepsilon_{tR}^2} + \frac{(2\varepsilon_{tR}^2-1)\varepsilon_L^3}{2(\varepsilon_{tR}^2+1)^3} + \dots \right) \psi_{L1}^t \end{aligned} \quad (3.26)$$

$$\begin{aligned} t_R &= t_R^1 \psi_{R1}^t + t_R^2 t_{R2} \\ &= \left( -\frac{\varepsilon_{tR}}{\sqrt{1+\varepsilon_{tR}^2}} + \frac{\varepsilon_{tR}\varepsilon_L^2}{(1+\varepsilon_{tR}^2)^{5/2}} + \dots \right) \psi_{R1}^t + \left( \frac{1}{\sqrt{1+\varepsilon_{tR}^2}} + \frac{\varepsilon_{tR}^2\varepsilon_L^2}{(1+\varepsilon_{tR}^2)^{5/2}} + \dots \right) t_{R2}, \end{aligned} \quad (3.27)$$

and similarly for the left- and right-handed  $b$ -quarks with  $\varepsilon_{tR} \rightarrow \varepsilon_{bR}$ . Here we denote the upper components of the  $SU(2)$  doublet fields as  $\psi_{L0,L1,R1}^t$ ; clearly the smaller the value of  $\varepsilon_L$  ( $\varepsilon_{tR}$ ), the more strongly the left-handed (right-handed) eigenstate will be concentrated at site 0 (site 2). Note that the relative phase of the eigenvectors  $t_L$  and  $t_R$  is set by the eigenstate condition

$$M_t^\dagger |t_L\rangle = m_t |t_R\rangle . \quad (3.28)$$

The left- and right-handed heavy fermion mass eigenstates are the orthogonal combinations

$$T_L = T_L^0 \psi_{L0}^t + T_L^1 \psi_{L1}^t \quad (3.29)$$

$$= \left( -\frac{\varepsilon_L}{1 + \varepsilon_{tR}^2} - \frac{(2\varepsilon_{tR}^2 - 1)\varepsilon_L^3}{2(\varepsilon_{tR}^2 + 1)^3} + \dots \right) \psi_{L0}^t + \left( -1 + \frac{\varepsilon_L^2}{2(1 + \varepsilon_{tR}^2)^2} + \frac{(8\varepsilon_{tR}^2 - 3)\varepsilon_L^4}{8(\varepsilon_{tR}^2 + 1)^4} + \dots \right) \psi_{L1}^t \quad (3.30)$$

$$T_R = T_R^1 \psi_{R1}^t + T_R^2 t_{R2} , \quad (3.31)$$

$$= \left( -\frac{1}{\sqrt{1 + \varepsilon_{tR}^2}} - \frac{\varepsilon_{tR}^2 \varepsilon_L^2}{(1 + \varepsilon_{tR}^2)^{5/2}} + \dots \right) \psi_{R1}^t + \left( -\frac{\varepsilon_{tR}}{\sqrt{1 + \varepsilon_{tR}^2}} + \frac{\varepsilon_{tR} \varepsilon_L^2}{(1 + \varepsilon_{tR}^2)^{5/2}} + \dots \right) t_{R2} , \quad (3.32)$$

and similarly for the left- and right-handed heavy  $B$  quarks with  $\varepsilon_{tR} \rightarrow \varepsilon_{bR}$ .

Analogous results follow for the other ordinary fermions and their heavy partners, with the appropriate  $\varepsilon_{fR}$  substituted for  $\varepsilon_{tR}$  in the expressions above.

## 4. Ideal Delocalization and $W$ Couplings

### 4.1 Ideal Delocalization

As shown in [32] it is possible to minimize precision electroweak corrections due to the light fermions by appropriate (“ideal”) delocalization of the light fermions along the moose. Essentially, if we recall that the  $W$  is orthogonal to its own heavy KK modes (the  $W'$  in the three-site model), then it is clear that relating the fermion profile along the moose appropriately to the  $W$  profile can ensure that the  $W'$  will be unable to couple to the fermions. Specifically, at site  $i$  we require the couplings and wavefunctions of the ideally delocalized fermion and the  $W$  boson to be related as

$$g_i (\psi_i^f)^2 = g_W v_W^i \quad (4.1)$$

In the three-site model, if we write the wavefunction of a delocalized left-handed fermion  $f_L = f_L^0 \psi_{L0}^f + f_L^1 \psi_{L1}^f$  then ideal delocalization imposes the following condition (having taken the ratio of the separate constraints for  $i = 0$  and  $i = 1$ ):

$$\frac{g(f_L^0)^2}{\tilde{g}(f_L^1)^2} = \frac{v_W^0}{v_W^1} . \quad (4.2)$$

Based on our general expressions for fermion mass eigenstates (eqns. (3.26) and (3.27)) and the  $W$  mass eigenstate (3.3), it is clear that (4.2) relates the flavor-independent quantities  $x$  and  $\varepsilon_L$  to the flavor-specific  $\varepsilon_{fR}$ . Hence, if we construe this as an equation for  $\varepsilon_L$  and solve perturbatively in the small quantity  $x$ , we find

$$\varepsilon_L^2 \rightarrow (1 + \varepsilon_{fR}^2)^2 \left[ \frac{x^2}{2} + \left( \frac{1}{8} - \frac{\varepsilon_{fR}^2}{2} \right) x^4 + \frac{5\varepsilon_{fR}^4 x^6}{8} + \dots \right]. \quad (4.3)$$

Regardless of the precise value of  $\varepsilon_{fR}$  involved, it is immediately clear that ideal delocalization implies  $\varepsilon_L = \mathcal{O}(x)$ . Since  $x \ll 1$ , this justifies the expansions used above in diagonalizing the fermion mass matrix.

The value of  $\varepsilon_L$  that yields precisely ideal delocalization for a given fermion species depends on  $\varepsilon_{fR}$  and therefore (3.23) on the fermion's mass. For example, the value of  $\varepsilon_L$  that ideally delocalizes the  $b$  depends on  $\varepsilon_{bR}$ . As we will see below, however, bounds on the right-handed  $Wtb$  coupling will yield the constraint  $\varepsilon_{bR} \leq 1.4 \times 10^{-2}$ ; when eqn. (4.3) is applied to the  $b$  quark and this constraint is imposed, terms proportional to  $\varepsilon_{bR}$  become negligible. As all other fermions (except top) are even lighter, the associated values of  $\varepsilon_{fR}$  will be even smaller. In practice, therefore, we may neglect all terms proportional to  $\varepsilon_{fR}$  in eqn. (4.3), and the condition for ideal mixing is essentially the same for all fermions except the top-quark:

$$\varepsilon_L^2 = \frac{x^2}{2} + \frac{x^4}{8} + \mathcal{O}(x^8) = 2 \left( \frac{M_W^2}{M_{W'}^2} \right) + 6 \left( \frac{M_W^2}{M_{W'}^2} \right)^2 + 22 \left( \frac{M_W^2}{M_{W'}^2} \right)^3 + \dots, \quad (4.4)$$

where the second equality follows from eqn. (3.6). This is the value of  $\varepsilon_L$  we will henceforth use for all fermions in our analysis. As discussed in [34], we expect that the value of  $x$  will be bounded by constraints on the  $WWZ$  vertex when the light fermions are ideally delocalized.

## 4.2 Left-handed $W$ couplings to Fermions

We may now compute the couplings between left-handed fermions (ordinary or heavy partners) and the light  $W$  boson. In terms of the mass-eigenstate gauge fields, the left-handed couplings of the light  $W$ 's may be written

$$\mathcal{L}_{WL} \propto W_\mu^+ [g v_W^0 (\bar{\psi}_{L0} \tau^- \gamma^\mu \psi_{L0}) + \tilde{g} v_W^1 (\bar{\psi}_{L1} \tau^- \gamma^\mu \psi_{L1})] + h.c. . \quad (4.5)$$

The couplings of the light- $W$  to the mass-eigenstate fermions is then computed by decomposing the gauge-eigenstate fermions into mass-eigenstates.

We begin with the left-handed  $Wtb$  coupling, assuming ideal mixing for the  $b$ -quark in the  $\varepsilon_{bR} \rightarrow 0$  limit. Because the  $W$  wavefunction receives contributions from sites 0 and 1 only, the  $Wff'$  coupling is the sum of the overlap between the  $W$  and fermion wavefunctions on those two sites:

$$g_L^{Wtb} = g t_L^0 b_L^0 v_W^0 + \tilde{g} t_L^1 b_L^1 v_W^1; \quad (4.6)$$

we find

$$g_L^{Wtb} = g \left( 1 - \frac{3\varepsilon_{tR}^4 + 4\varepsilon_{tR}^2 + 3}{8(\varepsilon_{tR}^2 + 1)^2} x^2 + \frac{3\varepsilon_{tR}^8 + 16\varepsilon_{tR}^6 + 50\varepsilon_{tR}^4 + 8\varepsilon_{tR}^2 + 15}{128(\varepsilon_{tR}^2 + 1)^4} x^4 + \dots \right). \quad (4.7)$$

The corresponding equation for the coupling of standard model fermions other than the top-quark to the  $W$  may be obtained by taking  $\varepsilon_{tR} \rightarrow 0$  in the equation above, yielding

$$g_L^W = g \left( 1 - \frac{3}{8} x^2 + \frac{15}{128} x^4 + \dots \right). \quad (4.8)$$

Combining this with eqns. (2.4), (3.2), (3.9), and (3.10) we find

$$g_L^W = \frac{e}{\sqrt{1 - \frac{M_W^2}{M_Z^2}}} [1 + \mathcal{O}(s^2 x^4)]. \quad (4.9)$$

which shows that the  $W$ -fermion couplings (for fermions other than top) are of very nearly standard model form, as consistent with ideal delocalization. Eqn. (4.8) corresponds to a value of  $G_F$

$$\sqrt{2}G_F = \frac{(g_L^W)^2}{4M_W^2} = \frac{1}{v^2} \left( 1 - \frac{x^2}{2} + \frac{x^4}{4} + \dots \right), \quad (4.10)$$

and the relation

$$g_L^{Wtb} = g_L^W \left( 1 + \frac{\varepsilon_{tR}^2}{4(\varepsilon_{tR}^2 + 1)^2} x^2 - \frac{\varepsilon_{tR}^2(3\varepsilon_{tR}^6 + 8\varepsilon_{tR}^4 + 4\varepsilon_{tR}^2 + 10)}{32(\varepsilon_{tR}^2 + 1)^4} x^4 + \dots \right). \quad (4.11)$$

The  $W$  also couples to the heavy partners of the ordinary fermions. Here, we quote the results for the  $T$  and  $B$  fermions; analogous results follow for other generations when  $\varepsilon_{tR}$  is replaced by the appropriate  $\varepsilon_{qR}$ . There is a diagonal  $WTB$  coupling of the form

$$g_L^{WTB} = gT_L^0 B_L^0 v_W^0 + \tilde{g}T_L^1 B_L^1 v_W^1, \quad (4.12)$$

$$= \frac{g}{2} \left( 1 - \frac{\varepsilon_{tR}^4 - 6\varepsilon_{tR}^2 - 5}{8(\varepsilon_{tR}^2 + 1)^2} x^2 + \dots \right) \quad (4.13)$$

$$= \frac{g_L^W}{2} \left( 1 + \frac{\varepsilon_{tR}^4 + 6\varepsilon_{tR}^2 + 4}{4(\varepsilon_{tR}^2 + 1)^2} x^2 + \dots \right), \quad (4.14)$$

where  $T_L^{0,1}$  and  $B_L^{0,1}$  are the heavy-fermion analogs of the components  $t_L^{0,1}$  and  $b_L^{0,1}$ . There are also smaller off-diagonal couplings involving one heavy and one ordinary fermion

$$g_L^{WTb} = gT_L^0 b_L^0 v_W^0 + \tilde{g}T_L^1 b_L^1 v_W^1, \quad (4.15)$$

$$= \frac{g(1 - \varepsilon_{tR}^2)}{2\sqrt{2}(\varepsilon_{tR}^2 + 1)} (x + \mathcal{O}(x^3)), \quad (4.16)$$

and

$$g_L^{WtB} = gt_L^0 B_L^0 v_W^0 + \tilde{g}t_L^1 B_L^1 v_W^1, \quad (4.17)$$

$$= \frac{g(1 + 2\varepsilon_{tR}^2)}{2\sqrt{2}(\varepsilon_{tR}^2 + 1)} (x + \mathcal{O}(x^3)), \quad (4.18)$$

which play an important role in radiative corrections.

### 4.3 Weak mixing angle

From Eqs. (3.9), (3.10) and (4.10) we can calculate the “ $Z$  standard” weak mixing angle  $\theta_W|_Z$ :

$$\begin{aligned} s_Z^2 c_Z^2 &\equiv \frac{e^2}{4\sqrt{2}G_F M_Z^2} \\ &= s^2 c^2 + s^2(c^2 - s^2) \left( c^2 - \frac{1}{4} \right) x^2 + O(x^4), \end{aligned} \quad (4.19)$$

where  $s_Z \equiv \sin \theta_W|_Z$  and  $c_Z \equiv \cos \theta_W|_Z$ . The relationship between the weak mixing angle  $\theta_W|_Z$  and the angle  $\theta$  defined in Eq. (2.4) is expressed as follows:

$$s_Z^2 = s^2 + \Delta, \quad c_Z^2 = c^2 - \Delta, \quad (4.20)$$

$$\Delta \equiv s^2 \left( c^2 - \frac{1}{4} \right) x^2 + O(x^4). \quad (4.21)$$

In other words,  $s_Z^2$  and  $s^2$  are the same up to corrections of order  $x^2$ .

### 4.4 Right-handed $W$ couplings and $b \rightarrow s\gamma$

Because  $\psi_R$  is a doublet under  $SU(2)_1$ , the three-site model includes a right-handed couplings of the  $W$

$$\mathcal{L}_{WR} \propto W_\mu^+ [\tilde{g} v_W^1 (\bar{\psi}_{R1} \tau^- \gamma^\mu \psi_{R1})] + h.c. . \quad (4.22)$$

Note that the right-handed fermions exist only sites 1 and 2 while the  $W$  is limited to sites 0 and 1; hence, the right-handed coupling comes entirely from the overlap at site 1. For the  $tb$  doublet we find

$$g_R^{Wtb} = \tilde{g} t_R^1 b_R^1 v_W^1 \quad (4.23)$$

$$= \frac{g}{2} \frac{\varepsilon_{tR}}{\sqrt{1 + \varepsilon_{tR}^2}} \frac{\varepsilon_{bR}}{\sqrt{1 + \varepsilon_{bR}^2}} (1 + \mathcal{O}(x^2)) \quad (4.24)$$

$$\approx \frac{g}{2} \frac{m_b}{m_t} \frac{\varepsilon_{tR}^2}{1 + \varepsilon_{tR}^2}, \quad (4.25)$$

where reaching the last line requires use of eqn. (3.23). It is interesting to note that this expression is precisely analogous to the related expression in the continuum model (see eqn. (4.17) of [29]).

The right-handed  $Wtb$  coupling can yield potentially large contributions to  $b \rightarrow s\gamma$ . As shown in [37], agreement with the experimental upper limit on this process requires

$$\frac{g_R^{Wtb}}{g_L^W} < 4 \times 10^{-3}. \quad (4.26)$$

Combining this bound with our expressions for  $g_L^W$  (4.8) and  $g_R^{Wtb}$  (4.25), recalling  $x \ll 1$ , and using  $m_t = 175$  GeV,  $m_b = 4.5$  GeV, yields the constraint

$$\varepsilon_{tR} < 0.67. \quad (4.27)$$

As we shall see below, this constraint will automatically be satisfied for  $M > 1.8$  TeV – a mass limit that will be shown to be required for consistency with top-quark mass generation and limits on  $\varepsilon_L$ . Finally, combining eqns. (4.27) and (3.23), reveals that

$$\varepsilon_{bR} < 1.4 \times 10^{-2} . \quad (4.28)$$

as referred to earlier. Again, this confirms that the same value of  $\varepsilon_L$  can produce nearly perfect ideal delocalization for the  $b$  and all of the lighter fermions.

The  $W$  also has right-handed couplings to  $T$  and  $B$ , for which we compute the diagonal coupling

$$g_R^{WTB} = \tilde{g} T_R^1 B_R^1 v_W^1 \quad (4.29)$$

$$= \frac{g}{2\sqrt{1 + \varepsilon_{tR}^2}} \left( 1 + \frac{\varepsilon_{tR}^4 + 6\varepsilon_{tR}^2 + 1}{8(\varepsilon_{tR}^2 + 1)^2} x^2 + \dots \right) \quad (4.30)$$

$$= \frac{g_L^W}{2\sqrt{1 + \varepsilon_{tR}^2}} \left( 1 + \frac{\varepsilon_{tR}^4 + 3\varepsilon_{tR}^2 + 1}{2(\varepsilon_{tR}^2 + 1)^2} x^2 + \dots \right) , \quad (4.31)$$

and the off-diagonal coupling

$$g_R^{WtB} = \tilde{g} t_R^1 B_R^1 v_W^1 \quad (4.32)$$

$$= \frac{g \varepsilon_{tR}}{2\sqrt{1 + \varepsilon_{tR}^2}} \left( 1 + \frac{\varepsilon_{tR}^4 + 2\varepsilon_{tR}^2 - 3}{8(\varepsilon_{tR}^2 + 1)^2} x^2 + \dots \right) \quad (4.33)$$

$$= \frac{g_L^W \varepsilon_{tR}}{2\sqrt{1 + \varepsilon_{tR}^2}} \left( 1 + \frac{\varepsilon_{tR}^2(\varepsilon_{tR}^2 + 2)}{2(\varepsilon_{tR}^2 + 1)^2} x^2 + \dots \right) . \quad (4.34)$$

As in the case of  $g_R^{Wtb}$ , the right-handed coupling  $g_R^{WTB}$  turns out to be proportional to  $\varepsilon_{bR}$ , and is therefore very small.

Other right-handed  $Wqq'$  couplings involving the light standard fermions are straightforward to deduce from eqn. (4.24) and clearly suppressed by the small values of  $\varepsilon_{qR}$ . Similarly, the off-diagonal  $g_R^{WQq'}$  are proportional to small  $\varepsilon_{qR}$ . The diagonal  $g_R^{WQQ'}$  are analogous in form to (4.31).

## 5. $Z$ Couplings to Fermions

The  $Z$  coupling to fermions may now be computed. Like the  $W$ , the  $Z$  may couple to a pair of ordinary or heavy-partner fermions, or to a mixed pair with one ordinary and one heavy-partner fermion. The left-handed coupling of the light  $Z$ -boson to quark fields may be written

$$\mathcal{L}_{ZL} \propto Z_\mu \left[ g v_Z^0 (\bar{\psi}_{L0} \frac{\tau^3}{2} \gamma^\mu \psi_{L0}) + \tilde{g} v_Z^1 (\bar{\psi}_{L1} \frac{\tau^3}{2} \gamma^\mu \psi_{L1}) + \frac{g'}{6} v_Z^2 (\bar{\psi}_{L0} \gamma^\mu \psi_{L0} + \bar{\psi}_{L1} \gamma^\mu \psi_{L1}) \right] , \quad (5.1)$$

where the first two terms give rise to the left-handed “ $T_3$ ” coupling and the last term (proportional to  $g'$ ) gives rise to the left-handed hypercharge coupling. The expression for leptons would be similar, replacing hypercharge  $1/6$  with  $-1/2$ .

Similarly, the right-handed coupling of the  $Z$  to quarks fields is

$$\mathcal{L}_{ZR} \propto Z_\mu \left[ \tilde{g} v_Z^1 (\bar{\psi}_{R1} \frac{\tau^3}{2} \gamma^\mu \psi_{R1}) + \frac{g'}{6} v_Z^2 (\bar{\psi}_{R1} \gamma^\mu \psi_{R1}) + g' v_Z^2 \left( \frac{2}{3} \bar{u}_{R2} \gamma^\mu u_{R2} - \frac{1}{3} \bar{d}_{R2} \gamma^\mu d_{R2} \right) \right] , \quad (5.2)$$

where the last three terms arise from the hypercharge. For leptons,  $1/6 \rightarrow -1/2$  in the second term,  $2/3 \rightarrow 0$  in the third term (for neutrinos), and  $-1/3 \rightarrow -1$  in the last term for the charged leptons. For quarks, this expression may be more conveniently rewritten as

$$\mathcal{L}_{ZR} \propto Z_\mu \left[ (\tilde{g} v_Z^1 - g' v_Z^2) (\bar{\psi}_{R1} \frac{\tau^3}{2} \gamma^\mu \psi_{R1}) + g' v_Z^2 \left( \frac{2}{3} \sum_{i=1,2} \bar{u}_{Ri} \gamma^\mu u_{Ri} - \frac{1}{3} \sum_{i=1,2} \bar{d}_{Ri} \gamma^\mu d_{Ri} \right) \right] , \quad (5.3)$$

where the last two terms yield the  $Z$ -couplings to the conventionally-defined right-handed hypercharge of the quarks, while the first can give rise to a new right-handed “ $T_3$ ” coupling.

### 5.1 $Z$ Couplings to Light Fermions

We now use eqns. (5.1) and (5.3) to compute the couplings of the  $Z$  to light fermions. For an ideally localized light fermion  $f$ , we find the left-handed coupling to  $T_3$  by summing the overlaps of the  $Z$  and fermion wavefunctions on sites 0 and 1 (the loci of the  $T_3$  charges):

$$g_{3L}^{Zqq} = g(f_L^0)^2 v_Z^0 + \tilde{g}(f_L^1)^2 v_Z^1 \quad (5.4)$$

$$= g c \left( 1 - \frac{x^2 c^2 (3 + 6t^2 - t^4)}{8} + \dots \right) \quad (5.5)$$

$$= \frac{eM_W}{M_Z \sqrt{1 - \frac{M_W^2}{M_Z^2}}} [1 + \mathcal{O}(s^2 x^4)] . \quad (5.6)$$

The coupling of left-handed light fermions to hypercharge arises from the overlap between the fraction of the  $Z$  wavefunction arising from site 2 (the locus of hypercharge) and the left-handed fermion wavefunctions which are limited to sites 0 and 1:

$$g_{YL}^{Zqq} = g' v_Z^2 [(f_L^0)^2 + (f_L^1)^2] = g' v_Z^2 \quad (5.7)$$

$$= -g' s \left( 1 + \frac{x^2 c^2 (3 - 2t^2 - t^4)}{8} + \dots \right) \quad (5.8)$$

$$= -\frac{eM_Z}{M_W} \sqrt{1 - \frac{M_W^2}{M_Z^2}} [1 + \mathcal{O}(s^2 x^4)] . \quad (5.9)$$

Equations (5.6) and (5.9), derived from the preceding equations using eqns. (2.4), (3.2), (3.9), and (3.10) show that the couplings are very nearly of standard model form; this is a further check of ideal delocalization.

Since the right-handed light fermion eigenvectors are localized entirely at site 2, there are no right-handed couplings of the light fermions to  $T_3$  and the right-handed hypercharge coupling of the  $Z$  is given by

$$g_{YR}^{Zqq} = g'v_Z^2(f_R^2)^2 = g'v_Z^2 = g_{YL}^{Zqq} , \quad (5.10)$$

where the last equality comes from eqn. (5.7).

For ideally delocalized light fermions, therefore, we find the  $Z$ -couplings are given by the standard-model like expression

$$\frac{eM_Z}{M_W \sqrt{1 - \frac{M_W^2}{M_Z^2}}} \left( T_3 P_L - \left( 1 - \frac{M_W^2}{M_Z^2} \right) Q \right) [1 + \mathcal{O}(s^2 x^4)] , \quad (5.11)$$

where  $P_L$  is the left-handed chirality projection operator.

## 5.2 $Z$ Couplings to the top and bottom

The left-handed coupling of the top-quark to  $T_3$  is

$$g_{3L}^{Ztt} = g(t_L^0)^2 v_Z^0 + \tilde{g}(t_L^1)^2 v_Z^1 \quad (5.12)$$

$$= g_{3L}^{Zqq} \left( 1 + \frac{\varepsilon_{tR}^2(2 + \varepsilon_{tR}^2)}{4c^2(1 + \varepsilon_{tR}^2)^2} x^2 + \dots \right) . \quad (5.13)$$

Note that a similar expression holds for the bottom quark, with  $\varepsilon_{tR} \rightarrow \varepsilon_{bR}$  and therefore, from eqn. (4.28), the tree-level corrections to the partial width  $\Gamma(Z \rightarrow b\bar{b})$  are proportional to  $\varepsilon_{bR}^2/2 < 0.01\%$ . From eqns. (5.1) and (5.3), we see that the left- and right-handed top-quark couplings to  $Y$  turn out to be the same as those for the other quarks

$$g_{YL}^{Ztt} = g'v_Z^2 [(t_L^0)^2 + (t_L^1)^2] = g_{YL}^{Zqq} \quad (5.14)$$

$$g_{YR}^{Ztt} = g'v_Z^2 [(t_R^1)^2 + (t_R^2)^2] = g_{YR}^{Zqq} . \quad (5.15)$$

We may also compute the right-handed  $T_3$  couplings of the top-quark

$$g_{3R}^{Ztt} = (\tilde{g}v_Z^1 - g'v_Z^2)(t_R^1)^2 \quad (5.16)$$

$$= \frac{g}{2c} \frac{\varepsilon_{tR}^2}{1 + \varepsilon_{tR}^2} (1 + \mathcal{O}(x^2)) . \quad (5.17)$$

The  $T_3$  couplings of the  $Z$  to a pair of heavy-partner fermions or an off-diagonal pair are given in Table 1. From the form of eqns. (5.1) and (5.3), we see that the hypercharge couplings of the  $Z$  to a pair of left-handed or right-handed heavy-partner fermions follow the pattern of the ordinary fermions:

$$g_{YR}^{ZQQ} = g'v_Z^2 = g_{YL}^{ZQQ} , \quad (5.18)$$

and the hypercharge coupling of the  $Z$  to an off-diagonal (flavor-conserving)  $Qq$  pair always vanishes

$$g_{YL}^{ZQq} = g_{YR}^{ZQq} = 0 \quad (5.19)$$

because the  $Q$  and  $q$  wavefunctions are orthogonal.

coupling	calculated as	strength
$g_{3L}^{Ztt}$	$g_0 v_Z^0 (t_L^0)^2 + g_1 v_Z^1 (t_L^1)^2$	$cg - \frac{1}{8}c^3 g(3 + 6t^2 - t^4) x^2 + \frac{g\varepsilon_{tR}^2(2+\varepsilon_{tR}^2)}{4c(1+\varepsilon_{tR}^2)^2} x^2$
$g_{3R}^{Ztt}$	$(g_1 v_Z^1 - g_2 v_Z^2)(t_R^1)^2$	$\frac{g\varepsilon_{tR}^2}{2c(\varepsilon_{tR}^2 + 1)} \left( 1 + \frac{-3(\varepsilon_{tR}^2 + 1)^2 + 8c^2 \varepsilon_{tR}^2 (\varepsilon_{tR}^2 + 2) - 4c^4 (\varepsilon_{tR}^2 + 1)^2}{8c^2 (\varepsilon_{tR}^2 + 1)^2} x^2 \right)$
$g_{3L}^{ZTT}$	$g_0 v_Z^0 (T_L^0)^2 + g_1 v_Z^1 (T_L^1)^2$	$-\frac{1}{2}cg (t^2 - 1) + \frac{cg(4(t^2+1)-c^2(\varepsilon_{tR}^2+1)^2(t^2-1)^3)}{16(\varepsilon_{tR}^2+1)^2} x^2$
$g_{3R}^{ZTT}$	$(g_1 v_Z^1 - g_2 v_Z^2)(T_R^1)^2$	$\frac{g}{2c(\varepsilon_{tR}^2+1)} + g \frac{(-3(\varepsilon_{tR}^2+1)^2+8c^2(\varepsilon_{tR}^4+3\varepsilon_{tR}^2+1)-4c^4(\varepsilon_{tR}^2+1)^2)}{16c^3(\varepsilon_{tR}^2+1)^3} x^2$
$g_{3L}^{ZtT}$	$g_0 v_Z^0 t_L^0 T_L^0 + g_1 v_Z^1 t_L^1 T_L^1$	$\frac{g}{2\sqrt{2}c(\varepsilon_{tR}^2+1)} x + g \frac{((\varepsilon_{tR}^2+1)^2+c^2(\varepsilon_{tR}^4+6\varepsilon_{tR}^2-3)-4c^4(\varepsilon_{tR}^2+1)^2)}{16\sqrt{2}c^3(\varepsilon_{tR}^2+1)^3} x^3$
$g_{3R}^{ZtT}$	$(g_1 v_Z^1 - g_2 v_Z^2) t_R^1 T_R^1$	$\frac{g\varepsilon_{tR}}{2c(\varepsilon_{tR}^2+1)} + g\varepsilon_{tR} \frac{(-3(\varepsilon_{tR}^2+1)^2+4c^2(2\varepsilon_{tR}^4+5\varepsilon_{tR}^2+1)-4c^4(\varepsilon_{tR}^2+1)^2)}{16c^3(\varepsilon_{tR}^2+1)^3} x^2$

**Table 1:** Strength of the  $T_3$  portion of the  $Z$  coupling to top flavored fermions in the three-site model to order  $x^3$ . The  $\varepsilon_{tR} \rightarrow \varepsilon_{fR}$  limit of a top-flavor coupling is the corresponding coupling of flavor  $f$ .

## 6. Multiple Gauge Boson Couplings and Chiral Lagrangian Parameters

### 6.1 $ZWW$ Vertex and $\Delta g_1^Z$

To leading order, in the absence of CP-violation, the triple gauge boson vertices may be written in the Hagiwara-Peccei-Zeppenfeld-Hikasa triple-gauge-vertex notation [38]

$$\begin{aligned}
\mathcal{L}_{TGV} = & -ie \frac{c_Z}{s_Z} [1 + \Delta\kappa_Z] W_\mu^+ W_\nu^- Z^{\mu\nu} - ie [1 + \Delta\kappa_\gamma] W_\mu^+ W_\nu^- A^{\mu\nu} \\
& - ie \frac{c_Z}{s_Z} [1 + \Delta g_1^Z] (W^{+\mu\nu} W_\mu^- - W^{-\mu\nu} W_\mu^+) Z_\nu \\
& - ie (W^{+\mu\nu} W_\mu^- - W^{-\mu\nu} W_\mu^+) A_\nu ,
\end{aligned} \tag{6.1}$$

where the two-index tensors denote the Lorentz field-strength tensor of the corresponding field. In the standard model,  $\Delta\kappa_Z = \Delta\kappa_\gamma = \Delta g_1^Z \equiv 0$ .

As noted in ref. [34], in any vector-resonance model, such as the Higgsless models considered here, the interactions (6.1) come from re-expressing the nonabelian couplings in the kinetic energy terms in the original Lagrangian in terms of the mass-eigenstate fields. In this case one obtains equal contributions to the deviations of the first and third terms, and the second and fourth terms in eqn. (6.1). In addition the coefficient of the fourth term is fixed by electromagnetic gauge-invariance, and therefore in these models we find

$$\Delta\kappa_\gamma \equiv 0 \quad \Delta\kappa_Z \equiv \Delta g_1^Z . \tag{6.2}$$

Computing the  $ZWW$  coupling explicitly in the three-site model yields

$$g_{ZWW} = g(v_W^0)^2 v_Z^0 + \tilde{g}(v_W^1)^2 v_Z^1 \quad (6.3)$$

$$= g c \left( 1 - \frac{x^2 c^2 (1 + 2t^2 - t^4)}{4} + \dots \right) \quad (6.4)$$

$$= e \frac{c_Z}{s_Z} \left( 1 + \frac{1}{8c^2} x^2 + O(x^4) \right) \quad (6.5)$$

$$= g_{3L}^{Zqq} \left( 1 + \frac{x^2}{8c^2} + \dots \right) . \quad (6.6)$$

where eqn. (6.5) is derived using (4.21). Hence we compute

$$\Delta g_1^Z = \Delta \kappa_Z = \frac{x^2}{8c^2} > 0 . \quad (6.7)$$

The 95% C.L. upper limit from LEP-II is  $\Delta g_1^Z < 0.028$  [39]. Approximating  $c^2 \approx \cos^2 \theta_W \approx 0.77$ , we find the bound on  $x$

$$x \leq 0.42 \sqrt{\frac{\Delta g_1^Z}{0.028}} , \quad (6.8)$$

and hence, from eqn. (3.5),

$$M_{W'} \approx \frac{2}{x} M_W \geq 380 \text{ GeV} \sqrt{\frac{0.028}{\Delta g_1^Z}} . \quad (6.9)$$

From eqn. (4.4), therefore, we can write

$$\varepsilon_L = \frac{m}{M} \approx \frac{x}{\sqrt{2}} \approx 0.30 \left( \frac{380 \text{ GeV}}{M_{W'}} \right) . \quad (6.10)$$

Finally, we recall that in the absence of a Higgs boson,  $W_L W_L$  spin-0 isospin-0 scattering would violate unitarity at a scale of  $\sqrt{8\pi}v$  and that exchange of the heavy electroweak bosons is what unitarizes  $WW$  scattering in higgsless models. Hence,  $M_{W'} \leq 1.2 \text{ TeV}$  in the three-site model. This constrains  $\varepsilon_L$  to lie in the range

$$0.095 \leq \varepsilon_L \leq 0.30 . \quad (6.11)$$

## 6.2 Quartic Gauge Boson Couplings

The  $WWWW$  coupling is calculated as follows.

$$\begin{aligned} g_{WWWW} &= g^2 (v_W^0)^4 + \tilde{g}^2 (v_W^1)^4, \\ &= g^2 \left( 1 - \frac{7}{16} x^2 + O(x^4) \right) \end{aligned} \quad (6.12)$$

Using eqn. (4.21) we may re-express this as

$$g_{WWWW} = \frac{e^2}{s_Z^2} \left( 1 + \frac{5}{16} x^2 + O(x^4) \right) . \quad (6.13)$$

We will use this in evaluating the Chiral Lagrangian parameters.

### 6.3 Longhitano's parameters

Of the complete set of 12 CP-conserving operators in the electroweak chiral Lagrangian written down by Longhitano [40, 41, 42, 43, 44, 45] and Appelquist and Wu [46], only five apply to Higgsless models such as the three-site model (see ref. [34] for a discussion):

$$\mathcal{L}_1 \equiv \frac{1}{2}\alpha_1 g_W g_Y B_{\mu\nu} \text{Tr}(TW^{\mu\nu}) \quad (6.14)$$

$$\mathcal{L}_2 \equiv \frac{1}{2}i\alpha_2 g_Y B_{\mu\nu} \text{Tr}(T[V^\mu, V^\nu]) \quad (6.15)$$

$$\mathcal{L}_3 \equiv i\alpha_3 g_W \text{Tr}(W_{\mu\nu}[V^\mu, V^\nu]) \quad (6.16)$$

$$\mathcal{L}_4 \equiv \alpha_4 [\text{Tr}(V^\mu V^\nu)]^2 \quad (6.17)$$

$$\mathcal{L}_5 \equiv \alpha_5 [\text{Tr}(V_\mu V^\mu)]^2. \quad (6.18)$$

Here  $W_{\mu\nu}$ ,  $B_{\mu\nu}$ ,  $T \equiv U\tau_3 U^\dagger$  and  $V_\mu \equiv (D_\mu U)U^\dagger$  are the basis of the expansion, with  $U$  being the nonlinear sigma-model field<sup>4</sup> arising from  $SU(2)_L \otimes SU(2)_R \rightarrow SU(2)_V$ . An alternative parametrization by Gasser and Leutwyler [47] names these coefficients as  $\alpha_1 = L_{10}$ ,  $\alpha_2 = -\frac{1}{2}L_{9R}$ ,  $\alpha_3 = -\frac{1}{2}L_{9L}$ ,  $\alpha_4 = L_2$ ,  $\alpha_5 = L_1$ .

The chiral Lagrangian coefficients are related<sup>5</sup> to  $\alpha S$ , the Hagiwara-Peccei-Zeppenfeld-Hikasa [38] triple-gauge-vertex parameters and the quartic  $W$  boson vertex as follows [34]:

$$\alpha S = -(16\pi\alpha) \alpha_1, \quad (6.19)$$

$$\Delta g_1^Z = \frac{1}{c^2(c^2 - s^2)} e^2 \alpha_1 + \frac{1}{s^2 c^2} e^2 \alpha_3, \quad (6.20)$$

$$\Delta \kappa_Z = \frac{2}{(c^2 - s^2)} e^2 \alpha_1 - \frac{1}{c^2} e^2 \alpha_2 + \frac{1}{s^2} e^2 \alpha_3, \quad (6.21)$$

$$g_{WWWW} = \frac{e^2}{s_Z^2} \left[ 1 + \frac{2}{(c^2 - s^2)} e^2 \alpha_1 + \frac{2}{s^2} e^2 \alpha_3 + \frac{1}{s^2} e^2 \alpha_4 \right]. \quad (6.22)$$

By solving the above equations with  $S = O(x^4)$  and with values of  $\Delta g_1^Z$ ,  $\Delta \kappa_Z$  and  $g_{WWWW}$  obtained earlier, we find

$$e^2 \alpha_1 = O(x^4), \quad (6.23)$$

$$e^2 \alpha_2 = -e^2 \alpha_3 = -\frac{s^2}{8} x^2 + O(x^4), \quad (6.24)$$

$$e^2 \alpha_4 = -e^2 \alpha_5 = \frac{s^2}{16} x^2 + O(x^4). \quad (6.25)$$

The coefficients  $\alpha_4$  and  $\alpha_5$  provide the leading corrections to  $WW$  and  $WZ$  elastic scattering. Note that the three-site model has  $\alpha_2 \neq \alpha_3$  and therefore,  $L_{9L} \neq L_{9R}$  [34, 45].

<sup>4</sup> $SU(2)_W \equiv SU(2)_L$  and  $U(1)_Y$  is identified with the  $T_3$  part of  $SU(2)_R$ .

<sup>5</sup> $\Delta \kappa_\gamma (= 0) = \frac{1}{s^2} (-e^2 \alpha_1 + e^2 \alpha_2 + e^2 \alpha_3)$  is automatically satisfied when  $\Delta g_1^Z = \Delta \kappa_Z$ .

	Three-site model	Continuum model
$\Delta g_1^Z = \Delta \kappa_Z$	$\frac{1}{2c^2} \left( \frac{M_W^2}{M_{W'}^2} \right)$	$\frac{\pi^2}{12c^2} \left( \frac{M_W^2}{M_{W'}^2} \right)$
$\Delta g_{WWWW}$	$\frac{5}{4} \left( \frac{M_W^2}{M_{W'}^2} \right)$	$\frac{\pi^2}{5} \left( \frac{M_W^2}{M_{W'}^2} \right)$
$e^2 \alpha_1$	0	0
$e^2 \alpha_2 = -e^2 \alpha_3$	$-\frac{s^2}{2} \left( \frac{M_W^2}{M_{W'}^2} \right)$	$-\frac{\pi^2 s^2}{12} \left( \frac{M_W^2}{M_{W'}^2} \right)$
$e^2 \alpha_4 = -e^2 \alpha_5$	$\frac{s^2}{4} \left( \frac{M_W^2}{M_{W'}^2} \right)$	$\frac{\pi^2 s^2}{30} \left( \frac{M_W^2}{M_{W'}^2} \right)$

**Table 2:** Quantities related to multi-gauge-boson vertices and chiral Lagrangian parameters in the three-site model and the continuum model of Ref [34].

## 6.4 Comparison to the Continuum Model

The three-site model may be viewed as an extremely deconstructed version of the model studied in ref. [34]: a five-dimensional flat-space  $SU(2)_A \otimes SU(2)_B$  gauge theory with ideally-delocalized fermions. Hence it is interesting to compare the values of the multiple gauge boson and chiral Lagrangian parameters obtained for the two cases.

The limit of the continuum model that is related to the three-site model has the bulk gauge couplings of  $SU(2)_A$  and  $SU(2)_B$ ,  $g_{5A}$  and  $g_{5B}$ , equal to one another; in the notation of ref. [34],  $\kappa = \frac{g_{5B}^2}{g_{5A}^2} = 1$ . Then, we may express both our values of the  $\alpha_i$  and those from ref. [34] in terms of the mass ratio  $M_W^2/M_{W'}^2$ , as shown in Table 2. Note that  $\Delta g_{WWWW}$  in the table is defined by

$$g_{WWWW} = \frac{e^2}{s_Z^2} [1 + \Delta g_{WWWW}]. \quad (6.26)$$

If we fix the value of  $\left( \frac{M_W^2}{M_{W'}^2} \right)$ , the quantities listed in Table 2 for the three-site model are about 70% as large as those for the continuum model.

## 7. Phenomenological Bounds

### 7.1 One-Loop Corrections to the $\rho$ Parameter

The existence of the new  $T$  and  $B$  fermions, the heavy partners of the top and bottom, give rise to new one-loop contributions to  $\Delta\rho$ , as illustrated in figure 2. In principle, it is the sum of the SM ( $t$  and  $b$  quark loops) and new physics contributions that is finite. However, we note that the SM contribution vanishes in the limit  $\varepsilon_L \rightarrow 0$  (and  $g' \rightarrow 0$ ) since the  $t$  and  $b$  quark masses are then equal (both vanish, per eqn. (3.21)). Since  $\varepsilon_L$  respects custodial symmetry, and fermionic custodial symmetry violation is encoded in the  $\varepsilon_{fR}$  coefficients, we may obtain the leading contribution to  $\Delta\rho$  from the new physics by performing the calculation

in the  $\varepsilon_L \rightarrow 0$  limit. We obtain

$$\Delta\rho \approx \frac{1}{16\pi^2} \frac{m_t^4}{M^2 v^2} = \frac{1}{16\pi^2} \frac{\varepsilon_{tR}^4 M^2}{v^2} . \quad (7.1)$$

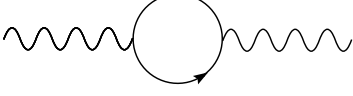


**Figure 2:** One-loop contributions to  $\Delta\rho$  arise from the differences in the vacuum polarization diagram for the  $W^3$  versus  $W^{1,2}$ . We compute the leading contribution in the limit  $\varepsilon_L \rightarrow 0$  and  $m_b \rightarrow 0$  (and  $g' \rightarrow 0$ ).

The phenomenological bounds on the value of  $\Delta\rho$  depend (since they include the one-loop standard model corrections) on the reference Higgs mass chosen. In the three site model, to leading-log approximation, the role of the Higgs boson is largely played by the  $W'$ . We are therefore interested in the bounds on  $\Delta\rho$  corresponding to Higgs masses between about 380 GeV (from eqn. (6.9)) and the unitarity bound 1.2 TeV. Current bounds (see, for example, Langacker and Erler in [48]) yield (approximately)  $\Delta\rho \leq 2.5 \times 10^{-3}$ , at 90% CL, assuming the existence of a moderately heavy (340 GeV) Higgs boson, while it is relaxed to approximately  $\Delta\rho \leq 5 \times 10^{-3}$  in the case of a heavy (1000 GeV) Higgs boson. We therefore expect that the upper bound on  $\Delta\rho$  in the three site model varies from approximately  $2.5 \times 10^{-3}$  and  $5 \times 10^{-3}$ . We may rewrite eqn. (7.1) as

$$\varepsilon_{tR} = 0.79 \left( \frac{\Delta\rho}{2.5 \times 10^{-3}} \right)^{1/4} \left( \frac{v}{M} \right)^{1/2} . \quad (7.2)$$

In what follows, we will quote limits on the parameters of the model for both of these values. For  $\Delta\rho = 5 \times 10^{-3}$ , we find the upper bound

$$\varepsilon_{tR} < 0.94 \left( \frac{v}{M} \right)^{1/2} . \quad (7.3)$$

As we shall see shortly, this bound is stronger than the one derived from  $b \rightarrow s\gamma$ .

## 7.2 Bounds on $M$

Our upper limit on  $\varepsilon_{tR}$  and our knowledge of the top quark mass allow us to derive a lower bound on  $M$ . Our expression (3.22) for  $m_t$  reminds us that

$$m_t \approx \frac{mm'_t}{\sqrt{M^2 + m_t^2}} = \frac{\varepsilon_L \varepsilon_{tR} M}{\sqrt{1 + \varepsilon_{tR}^2}} . \quad (7.4)$$

For a given value of  $M$ , the existence of an upper bound on  $\varepsilon_{tR}$  implies that there is a *smallest* allowed value of  $\varepsilon_L$ , which we denote  $\varepsilon_L^*$

$$\varepsilon_L^* = 1.26 \left( \frac{2.5 \times 10^{-3}}{\Delta\rho} \right)^{1/4} \frac{m_t}{\sqrt{vM}} \sqrt{1 + 0.63 \left( \frac{\Delta\rho}{2.5 \times 10^{-3}} \right)^{1/2} \frac{v}{M}} . \quad (7.5)$$

Since eqn. (6.11) requires  $\varepsilon_L^* < 0.30$ , for  $\Delta\rho = 2.5 \times 10^{-3}$  we find that  $M$  must be greater than 2.3 TeV, and for  $\Delta\rho = 5 \times 10^{-3}$  we find that  $M$  must be greater than 1.8 TeV.

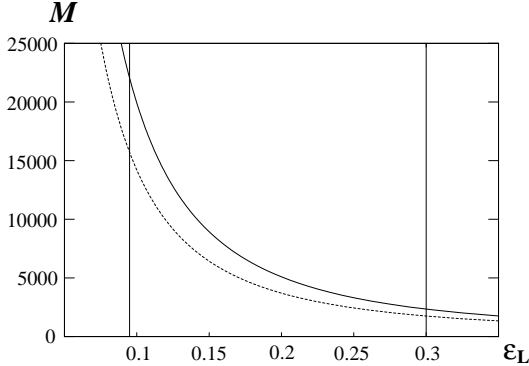


**Figure 3:** Phenomenologically acceptable values of  $M$  in GeV and  $\varepsilon_L$  for  $\Delta\rho = 2.5 \times 10^{-3}$  (solid curve) and  $5 \times 10^{-3}$  (dashed curve). The region bounded by the lines  $0.095 < \varepsilon_L < 0.30$ , and above the curves are allowed. For a given  $M$  and  $\varepsilon_L$ , the value of  $\varepsilon_{tR}$  is determined by eqn. (7.4). As discussed in the text, naive dimensional analysis implies  $M < 46$  TeV.

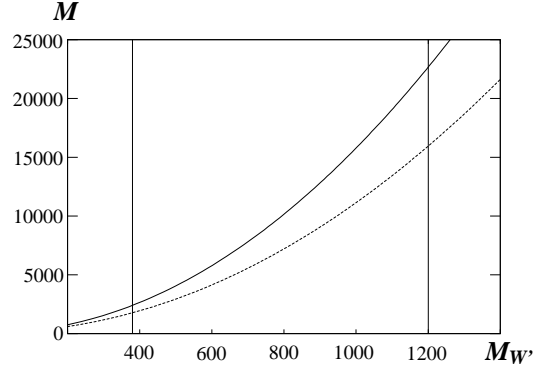


**Figure 4:** Phenomenologically acceptable values of  $M$  and  $M_{W'}$  in GeV for  $\Delta\rho = 2.5 \times 10^{-3}$  (solid curve) and  $5 \times 10^{-3}$  (dashed curve). The region bounded by the lines bounded by  $380 \text{ GeV} < M_{W'} < 1200 \text{ GeV}$  and above the curve are allowed. For a given  $M$  and  $M_{W'}$  (see eqn. (6.10)), the value of  $\varepsilon_{tR}$  is determined by eqn. (7.4). As discussed in the text, naive dimensional analysis implies  $M < 46$  TeV.

Several additional consequences follow. Using  $M > 1.8$  TeV and the bound in eqn. (7.3), we see that  $\varepsilon_{tR} < 0.35$ , which supersedes the  $b \rightarrow s\gamma$  constraint, eqn. (4.27), as promised above. For  $\Delta\rho = 2.5 \times 10^{-3}$ , as  $M$  grows above its minimum value of 2.3 TeV, according to eqn. (7.5) the value of  $\varepsilon_L^*$  will fall – reaching the lower bound of 0.095 (eqn. (6.11)) when  $M \approx 22$  TeV. For values of  $M$  greater than 22 TeV (and fixed  $m_t$ ), the entire range of  $0.095 < \varepsilon_L < 0.30$  remains accessible if  $\varepsilon_{tR}$  is smaller than its maximum value (which, for  $\Delta\rho = 2.5 \times 10^{-3}$ , is 0.26). The joint range of allowed  $\varepsilon_L$  and  $M$  for both values of  $\Delta\rho$  is summarized in figures 3 and 4.

In the simplest continuum models in which the 5th dimension is a flat interval, the mass of the first KK fermion resonance is approximately half of the mass of the first gauge-boson KK resonance. Due to the chiral boundary conditions on the fermions, Dirichlet at one boundary and Neumann at the other, the lowest KK fermion mode has a wavelength of twice the size of the 5-d interval. Phenomenologically, this situation is disfavored — and it has been suggested that this may be addressed by having the fermions “feel” a smaller size for the 5-d interval than the gauge-bosons [27, 29]. Following [29], the parameter which measures this enhancement is then given by

$$2 \frac{m_{t^*}}{M_{W'}}, \quad (7.6)$$

and, for the three-site model, we find the minimum value of is about 12 for  $\Delta\rho = 2.5 \times 10^{-3}$  and 7 for  $\Delta\rho = 5 \times 10^{-3}$ . In other words, viewing the three site model as the deconstruction of a continuum one, the bulk fermion fields behave as though the 5-d interval is at least twelve

or seven times smaller than do the gauge-bosons.

It is interesting to ask what *upper* bound exists on  $M$ . From the expression for the fermion mass matrix in eqns. (3.20) we have

$$M = \frac{\sqrt{2}\lambda v}{\varepsilon_L}. \quad (7.7)$$

Eqn. (6.11) requires  $\varepsilon_L \geq 0.095$ , and from naive dimensional analysis or, equivalently, perturbative unitarity, we expect  $\lambda \leq 4\pi$ . Hence,  $M < 46$  TeV. A more sophisticated analysis could be done by imposing unitarity of  $WW \rightarrow t\bar{t}$ , as in [29].

## 8. Decoupling and $Z \rightarrow b\bar{b}$ with a Toy UV Completion

In the analysis above we have argued that the “bulk fermion” Dirac mass  $M$  in the three site model must be large, between 1.8 and 46 TeV. Such a mass is potentially much larger than  $4\pi\sqrt{2}v \approx 4.3$  TeV, the largest mass which can arise from the symmetry breaking encoded by the link fields. By contrast, the nonlinear sigma model link fields have so far been described by an effective chiral lagrangian which is valid only at energies *less* than of order  $4\pi\sqrt{2}v$ . In order to discuss the three-site model in the large- $M$  limit, therefore, one must consider the question in the context of a theory which is consistent to much higher scales – *i.e.* a renormalizable one. The situation here is similar to the consistent analysis [49] of the Appelquist-Chanowitz bound [50].

The simplest possible renormalizable extension of the three site model is formed by promoting the link fields in figure 1 to linear sigma-model fields. Here one introduces two additional singlet fields  $H_i$  ( $i = 1, 2$ ) and considers the matrix fields

$$\Phi_i = \frac{(H_i + f_i)}{2} \Sigma_i, \quad (8.1)$$

which transform as  $(2, \bar{2})$  under the appropriate  $SU(2)$ 's, and which have the kinetic energy terms

$$\text{Tr} \left( D^\mu \Phi_i^\dagger D_\mu \Phi_i \right) \rightarrow \frac{1}{2} \partial^\mu H_i \partial_\mu H_i + \frac{f_i^2}{4} \text{Tr} \left( D^\mu \Sigma_i^\dagger D_\mu \Sigma_i \right). \quad (8.2)$$

The most general renormalizable potential for the fields  $\Phi_{1,2}$  will result in mixing between the fields  $H_{1,2}$ , which will therefore not be mass eigenstates. For the purposes of this note, however, this will not be relevant — we will require that, consistent with dimensional analysis, the masses of the “Higgs” are bounded by  $4\pi\sqrt{2}v$ .

For completeness, in this section we will carry the explicit dependence on  $f_{1,2}$ , although in practice we always have in mind  $f_1 \simeq f_2 \simeq \sqrt{2}v$  (as in eqn. (2.2)). We continue to work in the limit in which  $x = g_0/g_1 \ll 1$  and  $y = g_2/g_1 \ll 1$ .

In this linear sigma model version of the three-site model, the Yukawa couplings and fermion mass term are of the form below, which is the natural extension of eqn. (2.1)

$$\begin{aligned} \mathcal{L}_f = & \varepsilon_L M \left( 1 + \frac{H_1}{f_1} \right) \bar{\psi}_{L0} \Sigma_1 \psi_{R1} + M \bar{\psi}_{R1} \psi_{L1} + \\ & M \left( 1 + \frac{H_2}{f_2} \right) \bar{\psi}_{L1} \Sigma_2 \begin{pmatrix} \varepsilon_{uR} \\ \varepsilon_{dR} \end{pmatrix} \begin{pmatrix} u_{R2} \\ d_{R2} \end{pmatrix} + h.c. \end{aligned} \quad (8.3)$$

Although the Yukawa couplings are written in terms of the Dirac mass  $M$  for convenience, we do impose (see the discussion surrounding eqn. (7.7)) the consistency constraint

$$\frac{\varepsilon_L M}{f_1}, \quad \frac{(\varepsilon_{uR}, \varepsilon_{dR}) M}{f_2} < 4\pi, \quad (8.4)$$

on the size of the allowed Yukawa couplings.

## 8.1 The Large $M$ Effective Theory

We now consider the large- $M$  limit. Due to the decoupling theorem [51], the effects of the bulk (i.e. site-1) fermion on low-energy parameters must be suppressed by powers of  $M$ . Due to the parameterization of the couplings chosen in eqn. (8.3), the form of the operators in the low-energy effective theory may not obviously appear to be suppressed by  $M$  when written in terms of the parameters  $\varepsilon_L$  and  $\varepsilon_{uR,dR}$ . Nonetheless, because of the constraints of eqn. (8.4), the effects of the bulk fermion always formally decouple in the  $M \rightarrow \infty$  limit [51]. We will now look at light fermion masses, the coupling of delocalized light fermions to gauge bosons, and  $\Delta\rho$  in the large- $M$  limit and see how the results compare with our previous findings.

### 8.1.1 Light Fermion Masses

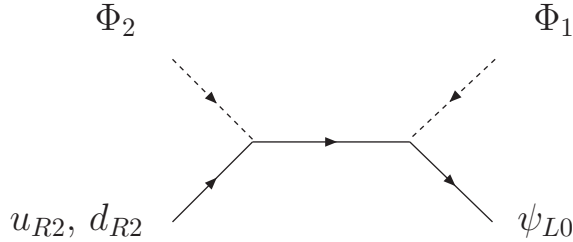


**Figure 5:** Mass-mixing diagram which yields the operator in eqn. (8.5) when integrating out the bulk fermion (interior fermion line) at tree-level.

The masses of the ordinary fermions arise in the large- $M$  limit when we consider the diagram connecting left-handed (site-0) and right-handed (site-2) brane fermions in fig. 1

and then integrate out the intervening site-1 bulk fermion at tree level. Specifically, this gives rise to the operator:

$$\mathcal{L}'_f \propto \frac{\varepsilon_L M}{f_1 f_2} \bar{\psi}_{L0} \Phi_1 \Phi_2 \begin{pmatrix} \varepsilon_{uR} & \\ & \varepsilon_{dR} \end{pmatrix} \begin{pmatrix} u_{R2} \\ d_{R2} \end{pmatrix} + h.c. . \quad (8.5)$$

$$\propto \varepsilon_L M \left(1 + \frac{H_1}{f_1}\right) \left(1 + \frac{H_2}{f_2}\right) \bar{\psi}_{L0} \Sigma_1 \Sigma_2 \begin{pmatrix} \varepsilon_{uR} & \\ & \varepsilon_{dR} \end{pmatrix} \begin{pmatrix} u_{R2} \\ d_{R2} \end{pmatrix} + h.c. . \quad (8.6)$$

In unitary gauge (with  $\Sigma_i = I$ ) the leading term provides the up-type fermion with a mass of the typical seesaw form  $m_u \propto \varepsilon_L \varepsilon_{uR} M$  that agrees with eqn. (3.21), and similarly for the down-type fermion. The overall power of  $M$  results from two powers of  $M$  in the Yukawa couplings, and one factor of  $1/M$  from the propagator in fig. 1.

### 8.1.2 Ideally Delocalized Fermion Couplings

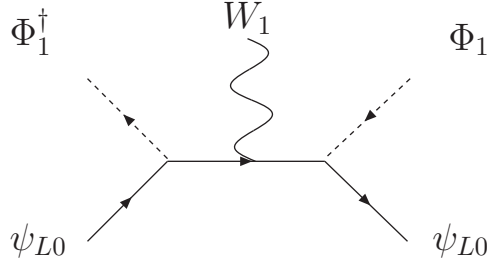


**Figure 6:** Coupling diagram which yields the operator in eqn. (8.7) when integrating out the bulk fermion at tree-level.

In this limit, it should also be possible to obtain an effective coupling of  $\psi_{L0}$  to the  $SU(2)$  group at site 1, consistent with light-fermion delocalization. Indeed, considering fig. 2 and integrating out the bulk fermion at tree-level induces the operator

$$\mathcal{L}'_{Wff} \propto \frac{\varepsilon_L^2}{f_1^2} \bar{\psi}_{L0} \Phi_1 i \not{D} \Phi_1^\dagger \psi_{L0} , \quad (8.7)$$

$$\supset \varepsilon_L^2 \bar{\psi}_{L0} \Sigma_1 i \not{D} \Sigma_1^\dagger \psi_{L0} , \quad (8.8)$$

which includes (easily visible in unitary gauge) just such an effective coupling. In this case, the two powers of  $M$  in the Yukawa couplings are cancelled by  $1/M^2$  from the fermion propagators in fig. 2. If we adjust the value of the coefficient  $\varepsilon_L$  to make the coupling of the light fermions to the  $W'$  vanish, we achieve ideal delocalization of the light fermions. The coupling of the brane fermions to the bulk gauge group is then precisely of the form discussed in section IIIB of [32].

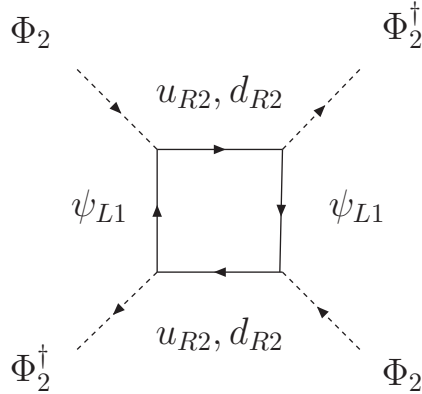


**Figure 7:** Loop Diagram giving the leading contribution to  $\Delta\rho$ , as encoded in the operator of eqn. (8.9).

### 8.1.3 Deviations in $\Delta\rho$

We may also check that the size of  $\Delta\rho$  in the large- $M$  limit is consistent with our previous calculation. As discussed in section 7.1, we expect that the leading contributions from beyond-the-standard-model physics will persist in the  $\varepsilon_L \rightarrow 0$  limit and will arise, in fact, from the weak isospin violation encoded in the  $\varepsilon_{fR}$ . Then the appropriate diagram<sup>6</sup> involves only the  $\bar{\psi}_{L1}\Phi_2(u_{R2},d_{R2})$  Yukawa couplings in eqn. (8.3) as shown in fig. 7, and gives rise to the operator<sup>7</sup>

$$\mathcal{L}'_{\Delta\rho} \propto \frac{M^2}{16\pi^2 f_2^4} \left( \text{Tr} \begin{pmatrix} \varepsilon_{uR}^2 & \\ & \varepsilon_{dR}^2 \end{pmatrix} \Phi_2^\dagger D^\mu \Phi_2 \right)^2, \quad (8.9)$$

$$\propto \frac{M^2}{16\pi^2} \left( \text{Tr} \begin{pmatrix} \varepsilon_{uR}^2 & \\ & \varepsilon_{dR}^2 \end{pmatrix} \Sigma_2^\dagger D^\mu \Sigma_2 \right)^2. \quad (8.10)$$

In unitary gauge, this may be seen to affect the mass of the  $Z$  and not that of the  $W$ . It encodes the very corrections to  $\Delta\rho$  discussed in section 7.1 and eqn. (7.1). Here the  $M^2$  arises from four powers of  $\varepsilon_R M$  from the couplings and an overall  $1/M^2$  from the convergent loop integral in the diagram.

## 8.2 $Z \rightarrow b\bar{b}$

With this background, we may now discuss flavor-dependent corrections to the process  $Z \rightarrow b\bar{b}$ . We will do so in the limit that  $m_b = 0$ , and hence  $\varepsilon_{bR} = 0$ . In the large- $M$  limit, therefore, we are interested in flavor-dependent corrections to the coupling of the lower-component of

<sup>6</sup>See [52] for a similar analysis in the case of the top-quark seesaw model.

<sup>7</sup>One may also deduce that this is the leading operator by recalling that  $\Delta\rho$  violates weak isospin by two units. An iso-triplet operator would not suffice.

$\psi_{L0}$  to the  $SU(2)_0$  gauge-bosons. Furthermore, as we are interested in flavor-nonuniversal contributions, we are only interested in couplings proportional to  $\varepsilon_{tR}$  — any contributions depending only on  $\varepsilon_L$  will be flavor-universal.

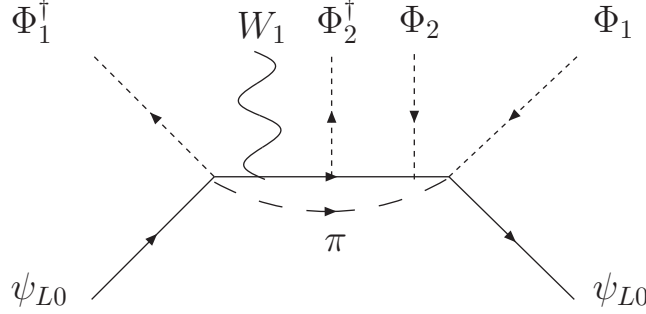


**Figure 8:** Loop Diagram giving leading contribution to the nonuniversal correction to  $Z \rightarrow b\bar{b}$ . Here  $\pi$  corresponds to a quantum charged “eaten” Goldstone boson, and the vertex involving the fermions,  $\Phi_1^\dagger$  and  $\pi$  is to be interpreted using “background field” method to preserve chiral invariance. This diagram, and those like it, give rise to the operator in eqn. (8.11) in the low-energy theory.

There are no relevant contributions at tree-level, as the neutral gauge-boson couplings involving  $\varepsilon_{tR}$  at tree-level couple to the upper component of  $\psi_{L0}$  — *i.e.* to the top-quark. The leading contributions arise from diagrams of the form shown in fig. 8. Note that the diagram involves the exchange of a charged Goldstone-boson (necessary to couple to the lower component of  $\psi_{L0}$ ), two couplings proportional to  $\varepsilon_L$  and two proportional to  $\varepsilon_{tR}$ . This diagram, and those like it, give rise to the low-energy operator

$$\mathcal{L}_{Zbb} \propto \frac{\varepsilon_L^2}{16\pi^2 f_1^2 f_2^2} \sum_a \bar{\psi}_{L0} \left[ \left( \frac{\tau^a}{2} \right) \Phi_1^\dagger \not{D} \Phi_2^\dagger \begin{pmatrix} \varepsilon_{uR}^2 & \\ & \varepsilon_{dR}^2 \end{pmatrix} \Phi_2 \Phi_1 \left( \frac{\tau^a}{2} \right) \right] \psi_{L0} . \quad (8.11)$$

Here four powers of  $M$  from the Yukawa couplings are cancelled by  $1/M^4$  from dimensional analysis.

An operator of this sort gives rise to a shift in the  $Zbb$  coupling of order

$$\frac{\delta g_{Zbb}}{g_{Zbb}^{SM}} \propto \frac{\varepsilon_L^2 \varepsilon_{tR}^2}{16\pi^2} = \frac{m_t^2}{16\pi^2 M^2} . \quad (8.12)$$

By contrast, the one-loop SM contribution to the  $Zb\bar{b}$  coupling [53, 54] is of order  $m_t^2/16\pi^2 v^2$ . We therefore see that the new corrections to the process  $Z \rightarrow b\bar{b}$  arising in the three site model are likely, even for the lowest possible  $M$ , to be negligibly small!<sup>6</sup>

In models with an extra dimension, one might generally be worried about effects which arise from integrating out the KK modes [56], as shown in fig. 9. Integrating out the heavy  $W'$  would lead one to anticipate a relatively large contribution of the form

$$\frac{\delta g_{Zbb}}{g_{Zbb}^{SM}} \simeq \frac{g^2 v^2}{16\pi^2 M_{W'}^2} \log \left( \frac{M_{W'}^2}{m_t^2} \right) . \quad (8.13)$$

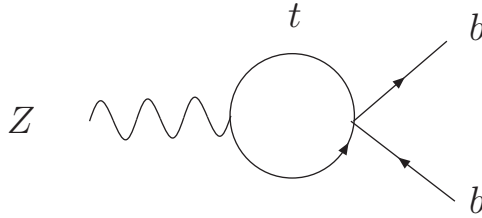


**Figure 9:** A potentially large correction to  $Z \rightarrow b\bar{b}$  in extra-dimensional models [56]. Due to ideal delocalization, however, the  $W'tb$  coupling vanishes, and this contribution is small in the three site model described here.

In a theory with ideal delocalization, however, the  $W'tb$  coupling vanishes, and therefore there is no such effect in the three site model described here.

We should also note that the estimate given above provides only a lower bound on the size of the corrections to the  $Zb\bar{b}$  coupling. It is possible that in a truly dynamical model, the “ETC”-like physics responsible for generating the Yukawa couplings can, themselves, give rise to new contributions [55].

Finally, it is worth mentioning that the situation could be somewhat different in a model with “Georgi fermions” [57]. In this case, all of the fermion masses arise from dimension-four Yukawa couplings so that it is not possible to take the large- $M$  limit, even in principle. Nonetheless, the analysis given here, taking the limit  $M \rightarrow \mathcal{O}(4\pi v)$ , shows that the effects on  $Z \rightarrow b\bar{b}$  are still likely to be quite small.

## 9. Conclusions

The three-site model is a useful tool for illustrating many issues of current interest in Higgsless models: ideal fermion delocalization, precision electroweak corrections, fermion mass generation, and phenomenological constraints. Because the Moose describing the model has only one “interior”  $SU(2)$  group, there is, accordingly, only a single triplet of  $W'$  and  $Z'$  states instead of the infinite tower of triplets present in the continuum limit. Likewise, there need only be single heavy fermion partner for each of the standard model fermions, instead of a tower of such states. Because the  $W'$  and  $Z'$  states are fermiophobic when the light fermions are ideally delocalized, discovering these heavy gauge bosons at a high-energy collider will require careful study of gauge-boson-fusion processes [34, 58]. Fortunately, the sparse spectrum and limited number of model parameters should allow this model to be encoded in a Matrix Event Generator program in concert with a Monte Carlo Event Generator for detailed phenomenological investigations.

In this paper, we have presented the forms of the gauge boson and fermion wavefunctions and their couplings to one another, and then explored the phenomenological implications. We established the form of the fermion Yukawa couplings required to produce the ideal fermion delocalization that causes tree-level precision electroweak corrections to vanish by making the

$W'$  and  $Z'$  fermiophobic. We computed the size of corrections to multi-gauge-boson vertices, found expressions for the electroweak chiral Lagrangian parameters, and compared these results to those obtained previously in the continuum limit. In addition, we have studied a variety of phenomenological constraints arising from anomalous gauge couplings, and from one-loop corrections to  $b \rightarrow s\gamma$  and the weak-isospin violating parameter  $\Delta\rho$ . We found that the extra fermiophobic vector boson states (the analogs of the gauge-boson KK modes in a continuum model) can be reasonably light, with a mass as low as 380 GeV, while the extra (approximately vectorial) quark and lepton states must satisfy  $1.8 \text{ TeV} \leq M \leq 46 \text{ TeV}$ .

Because the bulk fermion's Dirac mass  $M$  does not arise from electroweak symmetry breaking, its effects on low-energy parameters must decouple. To investigate this explicitly, we have constructed a large- $M$  effective field theory. Since  $M$  lies above the range of validity of the non-renormalizable non-linear sigma model for the link fields, our analysis employs the simplest possible UV completion, in which the link fields are given by renormalizable linear sigma models. This allows us to construct an effective low-energy theory produced when the bulk fermions of mass  $M$  are integrated out. We confirmed that the results in the large- $M$  effective theory for the top-quark mass, the gauge-boson couplings required by ideal delocalization, and the one-loop contribution to  $\Delta\rho$  are precisely those we computed directly. We then used the large- $M$  effective theory to estimate the size of the nonuniversal corrections to the  $Zb\bar{b}$  coupling – and found that these corrections can be very small, proportional to  $m_t^2/16\pi^2 M^2$ .

### Acknowledgments

R.S.C., E.H.S., B.C., and S.D. are supported in part by the US National Science Foundation under grant PHY-0354226. M.T.'s work is supported in part by the JSPS Grant-in-Aid for Scientific Research No.16540226. H.J.H. is supported by Tsinghua University. M.K. is supported in part by the US National Science Foundation under grant PHY-0354776.

### References

- [1] C. Csaki, C. Grojean, H. Murayama, L. Pilo and J. Terning, *Gauge theories on an interval: Unitarity without a Higgs*, Phys. Rev. D **69**, 055006 (2004) [arXiv:hep-ph/0305237].
- [2] P. W. Higgs, *Broken symmetries, massless particles and gauge fields*, Phys. Lett. **12** (1964) 132–133.
- [3] K. Agashe, A. Delgado, M. J. May and R. Sundrum, *RS1, Custodial Isospin and Precision Tests*, JHEP **0308**, 050 (2003) [arXiv:hep-ph/0308036].
- [4] C. Csaki, C. Grojean, L. Pilo, and J. Terning, *Towards a realistic model of higgsless electroweak symmetry breaking*, Phys. Rev. Lett. **92** (2004) 101802, [arXiv:hep-ph/0308038].
- [5] G. Burdman and Y. Nomura, *Holographic theories of electroweak symmetry breaking without a Higgs boson*, Phys. Rev. D **69**, 115013 (2004) [arXiv:hep-ph/0312247].

- [6] G. Cacciapaglia, C. Csaki, C. Grojean and J. Terning, *Oblique corrections from Higgsless models in warped space*, *Phys. Rev. D* **70**, (2004) 075014, [arXiv:hep-ph/0401160].
- [7] R. Sekhar Chivukula, D. A. Dicus, and H.-J. He, *Unitarity of compactified five dimensional yang-mills theory*, *Phys. Lett.* **B525** (2002) 175–182, [arXiv:hep-ph/0111016].
- [8] R. S. Chivukula and H.-J. He, *Unitarity of deconstructed five-dimensional yang-mills theory*, *Phys. Lett.* **B532** (2002) 121–128, [arXiv:hep-ph/0201164].
- [9] R. S. Chivukula, D. A. Dicus, H.-J. He, and S. Nandi, *Unitarity of the higher dimensional standard model*, *Phys. Lett.* **B562** (2003) 109–117, [arXiv:hep-ph/0302263].
- [10] H.-J. He, *Higgsless deconstruction without boundary condition*, arXiv:hep-ph/0412113.
- [11] R. Foadi, S. Gopalakrishna, and C. Schmidt, *Higgsless electroweak symmetry breaking from theory space*, *JHEP* **03** (2004) 042, [arXiv: hep-ph/0312324].
- [12] J. Hirn and J. Stern, *The role of spurions in Higgs-less electroweak effective theories*, *Eur. Phys. J. C* **34**, 447 (2004) [arXiv:hep-ph/0401032].
- [13] R. Casalbuoni, S. De Curtis and D. Dominici, *Moose models with vanishing  $S$  parameter*, *Phys. Rev. D* **70** (2004) 055010 [arXiv:hep-ph/0405188].
- [14] R. S. Chivukula, E. H. Simmons, H. J. He, M. Kurachi and M. Tanabashi, *The structure of corrections to electroweak interactions in Higgsless models*, *Phys. Rev. D* **70** (2004) 075008 [arXiv:hep-ph/0406077].
- [15] M. Perelstein, *Gauge-assisted technicolor?*, *JHEP* **10** (2004) 010, [arXiv:hep-ph/0408072].
- [16] H. Georgi, *Fun with Higgsless theories*, *Phys. Rev. D* **71**, 015016 (2005) [arXiv:hep-ph/0408067].
- [17] R. Sekhar Chivukula, E. H. Simmons, H. J. He, M. Kurachi and M. Tanabashi, *Electroweak corrections and unitarity in linear moose models*, *Phys. Rev. D* **71** (2005) 035007 [arXiv:hep-ph/0410154].
- [18] N. Arkani-Hamed, A. G. Cohen, and H. Georgi, *(de)constructing dimensions*, *Phys. Rev. Lett.* **86** (2001) 4757–4761, [arXiv:hep-th/0104005].
- [19] C. T. Hill, S. Pokorski, and J. Wang, *Gauge invariant effective lagrangian for kaluza-klein modes*, *Phys. Rev.* **D64** (2001) 105005, [arXiv:hep-th/0104035].
- [20] M. E. Peskin and T. Takeuchi, *Estimation of oblique electroweak corrections*, *Phys. Rev.* **D46** (1992) 381–409.
- [21] G. Altarelli and R. Barbieri, *Vacuum polarization effects of new physics on electroweak processes*, *Phys. Lett.* **B253** (1991) 161–167.
- [22] G. Altarelli, R. Barbieri, and S. Jadach, *Toward a model independent analysis of electroweak data*, *Nucl. Phys.* **B369** (1992) 3–32.
- [23] R. Barbieri, A. Pomarol, R. Rattazzi and A. Strumia, *Electroweak symmetry breaking after LEP1 and LEP2*, *Nucl. Phys. B* **703**, 127 (2004) [arXiv:hep-ph/0405040].
- [24] R. S. Chivukula, E. H. Simmons, H.-J. He, M. Kurachi, and M. Tanabashi, *Universal non-oblique corrections in higgsless models and beyond*, *Phys. Lett.* **B603** (2004) 210–218, [arXiv:hep-ph/0408262].

- [25] H. Georgi, *A tool kit for builders of composite models*, *Nucl. Phys.* **B266** (1986) 274.
- [26] G. Cacciapaglia, C. Csaki, C. Grojean and J. Terning, *Curing the ills of Higgsless models: The  $S$  parameter and unitarity*, *Phys. Rev. D* **71** (2005) 035015 [arXiv:hep-ph/0409126].
- [27] G. Cacciapaglia, C. Csaki, C. Grojean, M. Reece and J. Terning, *Top and bottom: A brane of their own*, *Phys. Rev. D* **72**, (2005) 095018 [arXiv:hep-ph/0505001].
- [28] R. Foadi, S. Gopalakrishna and C. Schmidt, *Effects of fermion localization in Higgsless theories and electroweak constraints*, *Phys. Lett. B* **606** (2005) 157 [arXiv:hep-ph/0409266].
- [29] R. Foadi and C. Schmidt, *An Effective Higgsless Theory: Satisfying Electroweak Constraints and a Heavy Top Quark*, *Phys. Rev. D* **73** (2006) 075011 [arXiv:hep-ph/0509071].
- [30] R. S. Chivukula, E. H. Simmons, H. J. He, M. Kurachi and M. Tanabashi, *Deconstructed Higgsless models with one-site delocalization*, *Phys. Rev. D* **71**, 115001 (2005) [arXiv:hep-ph/0502162].
- [31] R. Casalbuoni, S. De Curtis, D. Dolce and D. Dominici, *Playing with fermion couplings in Higgsless models*, *Phys. Rev. D* **71**, 075015 (2005) [arXiv:hep-ph/0502209].
- [32] R. Sekhar Chivukula, E. H. Simmons, H. J. He, M. Kurachi and M. Tanabashi, *Ideal fermion delocalization in Higgsless models*, *Phys. Rev. D* **72**, 015008 (2005) [arXiv:hep-ph/0504114].
- [33] R. Sekhar Chivukula, E. H. Simmons, H. J. He, M. Kurachi and M. Tanabashi, *Ideal fermion delocalization in five dimensional gauge theories*, *Phys. Rev. D* **72**, 095013 (2005) [arXiv:hep-ph/0509110].
- [34] R. S. Chivukula, E. H. Simmons, H. J. He, M. Kurachi and M. Tanabashi, *Multi-gauge-boson vertices and chiral Lagrangian parameters in higgsless models with ideal fermion delocalization*, *Phys. Rev. D* **72**, 075012 (2005) [arXiv:hep-ph/0508147].
- [35] C. Grojean, W. Skiba and J. Terning, *Disguising the oblique parameters*, *Phys. Rev. D* **73**, 075008 (2006) [arXiv:hep-ph/0602154].
- [36] C. T. Hill and A. K. Leibovich, *Natural theories of ultra-low mass PNCB's: Axions and quintessence*, *Phys. Rev. D* **66**, 075010 (2002) [arXiv:hep-ph/0205237].
- [37] F. Larios, M. A. Perez and C. P. Yuan, *Analysis of  $t b W$  and  $t t Z$  couplings from CLEO and LEP/SLC data*, *Phys. Lett. B* **457**, 334 (1999) [arXiv:hep-ph/9903394].
- [38] K. Hagiwara, R. D. Peccei, D. Zeppenfeld and K. Hikasa, *Probing The Weak Boson Sector In  $E^+ E^- \rightarrow W^+ W^-$* , *Nucl. Phys. B* **282**, 253 (1987).
- [39] The LEP Collaborations ALEPH, DELPHI, L3, OPAL and the LEP TGC Working Group. LEPEWWG/TC/2005-01; June 8, 2005.
- [40] T. Appelquist and C. W. Bernard, *Strongly Interacting Higgs Bosons*, *Phys. Rev. D* **22**, 200 (1980).
- [41] A. C. Longhitano, *Heavy Higgs Bosons In The Weinberg-Salam Model*, *Phys. Rev. D* **22**, 1166 (1980).
- [42] A. C. Longhitano, *Low-Energy Impact Of A Heavy Higgs Boson Sector*, *Nucl. Phys. B* **188**, 118 (1981).

- [43] T. Appelquist, *Broken Gauge Theories And Effective Lagrangians*, Print-80-0832 (YALE) *Based on lectures presented at the 21st Scottish Universities Summer School in Physics, St. Andrews, Scotland, Aug 10-30, 1980*
- [44] B. Holdom, *Corrections To Trilinear Gauge Vertices And  $e^+e^- \rightarrow W^+W^-$  In Technicolor Theories*, Phys. Lett. B **258**, 156 (1991).
- [45] A. F. Falk, M. E. Luke and E. H. Simmons, *Chiral lagrangians and precision measurements of triple gauge boson vertices at hadron colliders*, Nucl. Phys. B **365**, 523 (1991).
- [46] T. Appelquist and G. H. Wu, *The Electroweak chiral Lagrangian and new precision measurements*, Phys. Rev. D **48**, 3235 (1993) [arXiv:hep-ph/9304240].
- [47] J. Gasser and H. Leutwyler, *Chiral Perturbation Theory To One Loop*, Annals Phys. **158**, 142 (1984).
- [48] S. Eidelman *et al.* [Particle Data Group], Phys. Lett. B **592**, 1 (2004).
- [49] M. Golden, *Unitarity and fermion mass generation*, Phys. Lett. B **338**, 295 (1994) [arXiv:hep-ph/9408272].
- [50] T. Appelquist and M. S. Chanowitz, *Unitarity Bound On The Scale Of Fermion Mass Generation*, Phys. Rev. Lett. **59**, 2405 (1987) [Erratum-ibid. **60**, 1589 (1988)].
- [51] T. Appelquist and J. Carazzone, *Infrared Singularities And Massive Fields*, Phys. Rev. D **11**, 2856 (1975).
- [52] H. Collins, A. K. Grant and H. Georgi, *The phenomenology of a top quark seesaw model*, Phys. Rev. D **61**, 055002 (2000) [arXiv:hep-ph/9908330].
- [53] R. Barbieri, M. Beccaria, P. Ciafaloni, G. Curci and A. Vicere, *Radiative correction effects of a very heavy top*, Phys. Lett. B **288**, 95 (1992) [Erratum-ibid. B **312**, 511 (1993)] [arXiv:hep-ph/9205238].
- [54] R. Barbieri, M. Beccaria, P. Ciafaloni, G. Curci and A. Vicere, *Two loop heavy top effects in the Standard Model*, Nucl. Phys. B **409**, 105 (1993).
- [55] R. S. Chivukula, S. B. Selipsky and E. H. Simmons, *Nonoblique effects in the  $Z b$  anti- $b$  vertex from ETC dynamics*, Phys. Rev. Lett. **69**, 575 (1992) [arXiv:hep-ph/9204214].
- [56] J. F. Oliver, J. Papavassiliou and A. Santamaria, *Universal extra dimensions and  $Z \rightarrow b$  anti- $b$* , Phys. Rev. D **67**, 056002 (2003) [arXiv:hep-ph/0212391].
- [57] H. Georgi, *Chiral fermion delocalization in deconstructed Higgsless theories*, arXiv:hep-ph/0508014.
- [58] A. Birkedal, K. Matchev and M. Perelstein, *Collider phenomenology of the Higgsless models*, Phys. Rev. Lett. **94**, 191803 (2005) [arXiv:hep-ph/0412278].